(Table 1), separated PCR products using electrophoregram, purified them and sequenced them using the process described above.

Results and discussion

We amplified all *F9* exons and intron–exon junctions of the patient's DNA using *F9*-specific PCR primers. We were able to obtain accurately amplified products and confirm normal DNA sequences, except for exon 6. The results of exon 6-specific PCR (Fig. 1a) and long-range PCR through exon 5 to exon 6 (Fig. 1b) showed PCR products more than 2-kb larger than that of the normal control. We also performed multiplex ligation-dependent probe amplification (MLPA) to analyze the relative gene dosage values for all *F9* exons from the patient as previously described [6], and found an absence of intragenic deletions or duplications in the *F9* regions targeted by the designed probes (data not shown). These data revealed a large insertion located at the intron 5–exon 6 junction without causative mutation in any other *F9* exon, suggesting that the exon 6 insertion is responsible for deficiency of the FIX activity observed in the patient.

To sequence the entire exon 6 insertion present in the proband, we prepared variable-length deletion inserts using Exonuclease III and S1 nuclease and determined their sequences. This allowed us to identify a 2,524-bp insertion flanked on both sides by an identical 15-bp sequence (5′-TTCTAGTGCCATTTC-3′), which was intron 5–exon 6 boundary of *F9* (Fig. 2a, Supplementary data). The insertion contained a 28-bp poly-T tract at the 5′ end, a GC-rich region, 18 hexamer (AGAGGG) repeats and additional AGAGC residues at the 3′ end. These features characterize an SVA retrotransposon in the antisense orientation and classify the retrotransposon in SVA family F with 15-bp target site duplications (TSDs), according to RepeatMasker (http://www.repeatmasker.org/) (Fig. 2b, c).

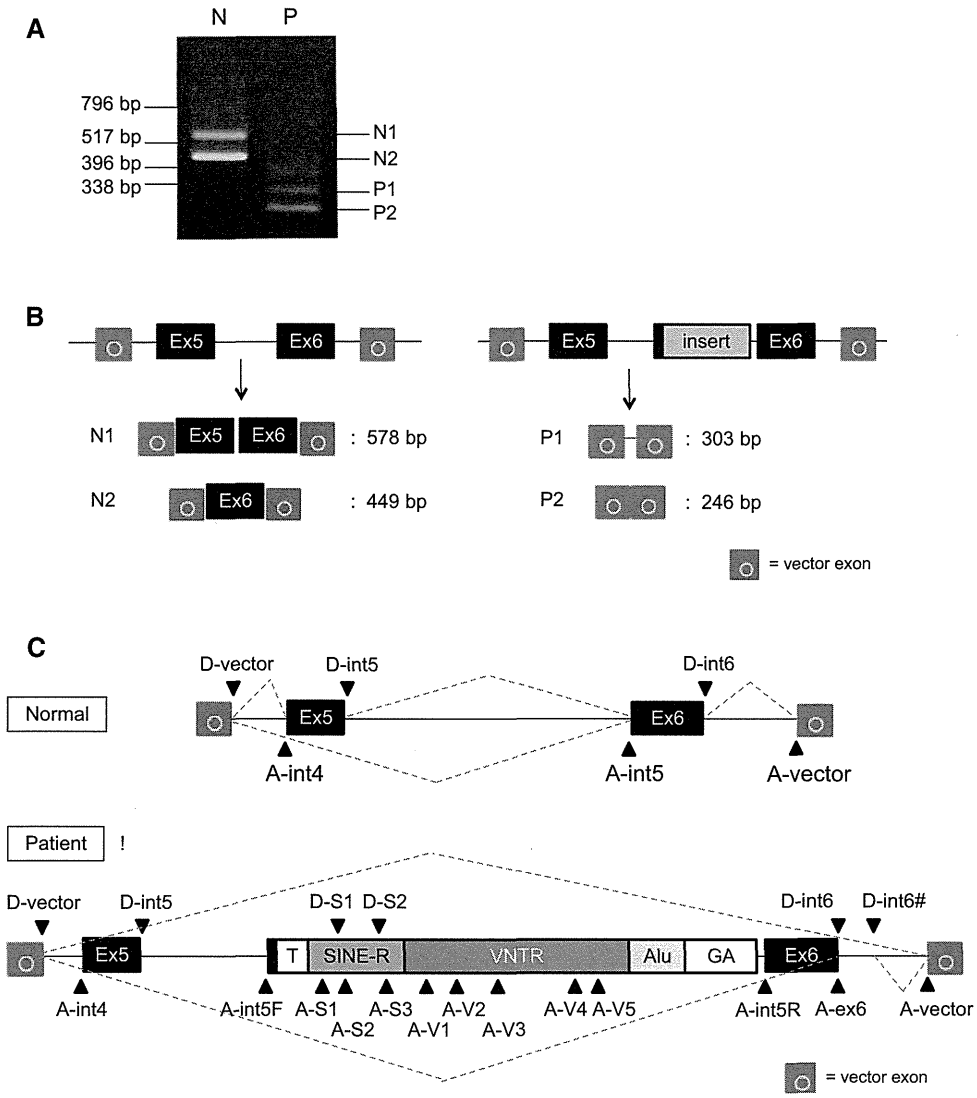

Fig. 3 Exontrap analysis. **a** Results of RT-PCR. In normal lane (*N*), 578-bp (*N1*) and 449-bp (*N2*) amplicons were observed. In patient lane (*P*), 303-bp (*P1*) and 246-bp (*P2*) amplicons were observed. **b** Schematic diagram of amplicon composition. The 578-bp (*N1*) amplicon resulted from trapping exons 5 and 6, whereas the 449-bp (*N2*) amplicon trapped only exon 6. The 303-bp fragment (*P1*) resulted from exon skipping together with trapping of a 57-bp sequence of intron 6 (c.723 + 1_57), whereas the 246-bp amplicon (*P2*) resulted from no trapping. **c** Predicted splice sites in the exontrap construct, with and without SVA. *Downward-pointing triangles* indicate splice-donor sites and *upward-pointing triangles* indicate splice-acceptor sites, according to splice site prediction tools (BDGP: Splice Site Prediction by Neural Network). *Dashed lines* denote observed splicing events

The human genome contains active retrotransposons such as human endonuclease retrovirus (HERV), long interspersed nucleotide elements (LINEs) and short interspersed nucleotide elements (SINEs). There is a smaller retrotransposon family known as SVA (SINE-VNTR-Alu) consisting of SINE, variable number of tandem repeats (VNTRs) and Alu-like sequences, which remains active in the human genome and capable of inducing disease-causing insertions [8].

SVA retrotransposons are increasing in the human genome, even though these elements lack independent mobilization. L1, the only autonomously active retrotransposon, encodes an internal RNA polymerase (pol II) promoter, an RNA binding protein, an endonuclease and a reverse transcriptase [9]. Experimental evidence indicates that SVA retrotransposons are mobilized by L1 elements in human cultured cells [10]. For this reason, SVA elements are considered non-autonomous retrotransposons that are mobilized by L1-encoded machinery *in trans*.

The copy numbers of retrotransposons in the human genome have been estimated as 516,000 for L1, 1,100,000 for Alu and 2700 for SVA [8]. Retrotransposition frequencies per birth were calculated as 1 in 21 for L1, 1 in 108 for Alu and 1 in 916 for SVA. These transposition events may affect individual phenotype like single nucleotide polymorphisms (SNPs) or copy number variations (CNVs), and cause disease in some cases. A recent report finds 96 retrotransposition events resulting in single-gene diseases, including 25 cases of L1, 60 cases of Alu, 4 cases of poly-A and 7 cases of SVA [11]. Callinan and Batzer [12] reported that retrotransposition events caused about 0.27 % of all human disease and can produce insertions, deletions, genomic rearrangements and recombination between homologous elements. The seven SVA insertions were SVA-F or SVA-E retrotranspositions arranged in sense orientation, except in one case [13]. Analysis of mRNA indicated that the six SVA insertions occurring in sense orientation, regardless of whether they were located in an exon or an intron, caused exon skipping or exonization of SVA using a cryptic splice site within the SVA element; these resulted in several diseases, such as Fukuyama-type congenital muscular dystrophy (FCMD), X-linked agammaglobulinemia and autosomal recessive hypercholesterolemia (ARH) [14–16]. However, an antisense-orientated SVA retrotransposition detected in intron 32 of the TATA box binding protein-associated factor 1 (TAF1) gene showed reduced mRNA or protein levels [17]. SVA elements are likely to be hypermethylated due to their high GC content and the large number of CpG sites they contain.

Table 2 Splice prediction scores

Region	Name	Score	5′–3′ sequence
A. Normal			
Donor site			
Intron 5 splice	D-int5	<0.4	CCAGCAG **gt**cataat
Intron 6 splice	D-int6	0.79	TTGGCAG **gt**acttta
Acceptor site			
Intron 4 splice	A-int4	0.94	gtagttccatgtacttttt**ag** ATGTAACATGTAACA
Intron 5 splice	**A-int5**	**0.99**	atttttcttctatttttct**ag** TGCCATTTCCATGTG
B. With SVA insertion			
Donor site			
In SINE-R	D-S1	0.93	AGGGAAG **gt**cagtag
In SINE-R	D-S2	0.93	GTTGGGG **gt**aaggtc
In intron 6	D-in6#	0.58	AGGCCAG **gt**gggaga
Acceptor site			
Intron 5 F	**A-in5F**	**0.98**	atttttcttctatttttct**ag** TGCCATTTCTTTTTT
In SINE-R	A-S1	0.92	attcttgggtgtttctcac**ag** AGGGGGATTTGGCAG
In SINE-R	A-S2	0.89	aaaggtctctggttttcct**ag** GCAGAGGACCCTGCG
In SINE-R	A-S3	0.92	tgtctacttctttctacac**ag** ACACGGCAACCATCC
In VNTR	A-V1	0.84	cgcccctcacctcccggac**ag** GGCGGCTGGCCGGGC
In VNTR	A-V2	0.96	ccccacctccctcccggac**ag** GGCGGCTGGCGGGCG
In VNTR	A-V3	0.89	gagatgctcctca cttccc **ag** ATG G G GTG G CTG CCG
In VNTR	A-V4	0.8	gagacgctcctcacttcct**ag** ATGTGATGGCGGCCG
In VNTR	A-V5	0.94	gaggtgctcctcacttcct**ag** ATGGGATGGCGGCCG
In VNTR	A-V6	0.89	gagacactcctcccttccc**ag** ACG G G GTG GCG GCCG
Intron 5 R	**A-int5R**	**<0.4**	gagggagagggagacttct**ag** TGCCATTTCCATGTG
In exon 6	A-ex6	0.81	ccaggtcaattcccttggc**ag** GTACTTTATACTGAT

D donor, *A* acceptor, *F* forward, *R* rear

Capital/small letter, exon/intron; bold letter, **gt**(donor)-**ag**(acceptor) splicing recognition sequences; under line, 15-bp target site duplication (TSD)

In the exontrap analysis, the cDNA sample from the vector of a normal individual showed a 578-bp amplicon consisting of exons 5 and 6 and a 449-bp amplicon consisting of exon 6; in both cases, the *F9* exons were flanked by the vector exons. In contrast, the cDNA sample from the patient produced abnormal 303-bp and 246-bp amplicons. Direct sequence analysis showed that the smaller amplicon consisted of only vector exons and the larger one contained a 57-bp sequence from intron 6 (c.723 + 1_57) flanked by vector exons (Fig. 3a, b). These results suggest that this insertion could disrupt regular splicing at exons 5 and 6. According to splice site prediction tools (BDGP: Splice Site Prediction by Neural Network, http://www.fruitfly.org/seq_tools/splice.html/), the prediction score of the splice-donor site in intron 5 (D-int5) was <0.4, suggesting that the procedure successfully trapped exon 6 in the normal cDNA sample (Table 2). The SVA insertion in exon 6 dramatically lowered the prediction score of the downstream intron 5 splice-acceptor site (A-int5R) in the rear 15-bp duplication and newly introduced multiple predicted splice sites (Table 2). It also resulted in an aberrant trapped transcript consisting of a 57-bp sequence of intron 6 (c.723 + 1_57), using A-ex6 as a splice-acceptor site and D-int6# as a splice-donor site (Fig. 3c; Table 2).

So far, there have been five reports of retrotranspositions in *F9*, of which three were of Alu insertions and two were of LINE-1 (L1) insertions [11]. These cases all involve insertions in exons and are predicted to cause frameshifting of *F9* mRNA and premature termination of the FIX protein. However, the causative mechanism for hemophilia B remains unknown because mRNA analysis has not been performed. It is possible that these cases involve exon skipping or exonization due to the presence of cryptic splice sites in the transposed elements. In this study, we detected a TSD at the intron 5–exon 6 boundary of *F9*, locating the SVA retrotransposon at the beginning of exon 6. We performed exontrap analysis to detect abnormal splicing and confirmed the disturbance of regular splicing of exons 5 and 6 due to the SVA retrotransposon located in the antisense strand. Although this analysis could not precisely replicate in vivo splicing conditions, it is suggested that exon skipping or exonization using unusual splice sites may result in reduced FIX levels via nonsense-mediated mRNA decay [18].

In conclusion, we identified an SVA-F retrotransposon associated with abnormal splicing in exon 6 of *F9* from a Japanese hemophilia B patient. This is the first report of SVA retrotransposition in *F9* causing severe hemophilia B.

Acknowledgments The authors thank Ms. C. Wakamatsu for her expert technical assistance and Ms. M. Goto for data collection. This study was financially supported in part by the Japanese Ministry of Education, Culture, Sports, Science, and Technology Subsidy Program (25293129: T. Kojima) and the Japanese Ministry of Health, Labour and Welfare Research Subsidy Program (T. Kojima and M. S.). The authors would like to thank Enago (www.enago.jp) for the English language review.

Conflict of interest The authors declare that they have no conflict of interest.

References

1. Yoshitake S, Schach BG, Foster DC, Davie EW, Kurachi K. Nucleotide sequence of the gene for human factor IX (antihemophilic factor B). Biochemistry. 1985;24:3736–50.
2. Bolton-Maggs PHB, Pasi KJ. Haemophilias A and B. Lancet. 2003;361:1801–9.
3. Li T, Miller CH, Payne AB, Craig Hooper W. The CDC hemophilia B mutation project mutation list: a new online resource. Mol Genet Genomic Med. 2013;1:238–45.
4. Kojima T, Tanimoto M, Kamiya T, Obata Y, Takahashi T, Ohno R, et al. Possible absence of common polymorphisms in coagulation factor IX gene in Japanese subjects. Blood. 1987;69:349–52.
5. Okumura K, Fujimori Y, Takagi A, Murate T, Ozeki M, Yamamoto K, et al. Skewed X chromosome inactivation in fraternal female twins results in moderately severe and mild haemophilia B. Haemophilia. 2008;14:1088–93.
6. Kato I, Takagi Y, Ando Y, Nakamura Y, Murata M, Takagi A, et al. A complex genomic abnormality found in a patient with antithrombin deficiency and autoimmune disease-like symptoms. Int J Hematol. 2014;100:200–5.
7. Takagi A, Kojima T, Tsuzuki S, Katsumi A, Yamazaki T, Sugiura I, et al. Structural organization and promoter activity of the human ryudocan gene. J Biochem. 1996;119:979–84.
8. Lander ES, Linton LM, Birren B, Nusbaum C, Zody MC, Baldwin J, et al. Initial sequencing and analysis of the human genome. Nature. 2001;409:860–921.
9. Beck CR, Collier P, Macfarlane C, Malig M, Kidd JM, Eichler EE, et al. LINE-1 retrotransposition activity in human genomes. Cell. 2010;141:1159–70.
10. Raiz J, Damert A, Chira S, Held U, Klawitter S, Hamdorf M, et al. The non-autonomous retrotransposon SVA is trans-mobilized by the human LINE-1 protein machinery. Nucleic Acids Res. 2012;40:1666–83.
11. Hancks DC, Kazazian HH. Active human retrotransposons: variation and disease. Curr Opin Genet Dev. 2012;22:191–203.
12. Callinan PA, Batzer MA. Retrotransposable elements and human disease. Genome Dyn. 2006;1:104–15.
13. Kaer K, Speek M. Retroelements in human disease. Gene. 2013;518:231–41.
14. Taniguchi-Ikeda M, Kobayashi K, Kanagawa M, Yu CC, Mori K, Oda T, et al. Pathogenic exon-trapping by SVA retrotransposon and rescue in Fukuyama muscular dystrophy. Nature. 2011;478:127–31.
15. Conley ME, Partain JD, Norland SM, Shurtleff SA, Kazazian HH. Two independent retrotransposon insertions at the same site within the coding region of BTK. Hum Mutat. 2005;25:324–5.
16. Wilund KR, Yi M, Campagna F, Arca M, Zuliani G, Fellin R, et al. Molecular mechanisms of autosomal recessive hypercholesterolemia. Hum Mol Genet. 2002;11:3019–30.
17. Makino S, Kaji R, Ando S, Tomizawa M, Yasuno K, Goto S, et al. Reduced neuron-specific expression of the TAF1 gene is associated with X-linked dystonia-parkinsonism. Am J Hum Genet. 2007;80:393–406.
18. Hancks DC, Ewing AD, Chen JE, Tokunaga K, Kazazian HH. Exon-trapping mediated by the human retrotransposon SVA. Genome Res. 2009;19:1983–91.

Haemophilia
The Official Journal of the World Federation of Hemophilia,
European Association for Haemophilia and Allied Disorders and
the Hemostasis & Thrombosis Research Society

Haemophilia (2015), 1–7 DOI: 10.1111/hae.12849

ORIGINAL ARTICLE

Distinct X chromosomal rearrangements in four haemophilia B patients with entire *F9* deletion

Y. NAKAMURA,* Y. ANDO,* Y. TAKAGI,* M. MURATA,*† T. KOZUKA,* Y. NAKATA,* R. HASEBE,* A. TAKAGI,* T. MATSUSHITA,‡ M. SHIMA§ and T. KOJIMA*

**Department of Pathophysiological Laboratory Sciences, Nagoya University Graduate School of Medicine, Nagoya; †Japan Society for the Promotion of Science, Tokyo; ‡Department of Transfusion Medicine, Nagoya University Hospital, Nagoya; and §Department of Paediatric, Nara Medical University, Nara, Japan*

Introduction: Haemophilia B is an X-linked bleeding disorder caused by a coagulation factor IX gene (*F9*) abnormality. Numerous *F9* defects have been identified to date; however, only a few with an entire *F9* deletion have been reported in detail. **Aim:** To elucidate the cause of severe haemophilia B, we investigated the precise X chromosome abnormalities in four Japanese patients who did not show all amplifications in *F9*-specific PCR. **Methods:** We analysed the patient's genomic DNA using Multiplex ligation-dependent probe amplification (MLPA). To assess the extent of any deletions, we further performed mapping PCRs, inverse PCRs or long-range PCRs and direct sequencing analyses of the X chromosome. **Results:** We detected entire *F9* deletions in four haemophilia B patients and identified the precise deleted regions of the X chromosome including *F9*. Patient 1 had a 149-kb deletion with breakpoints 90-kb upstream and 30-kb downstream from *F9*. Patients 2 and 3 showed 273-kb and 1.19-Mb deletions respectively. Patient 4 had two deleted regions: a 1663-bp deletion 1.34-Mb upstream from *F9* and a 7.2-Mb deletion including *F9*. These distinct breakpoints found in four different patients suggest that the mechanism of X chromosome deletion may be different between individuals. Non-allelic homologous recombination (NAHR), microhomology-mediated break-induced replication (MMBIR) or fork stalling and template switching (FoSTeS) may occur in respective X chromosomes of the four haemophilia B patients analysed. **Conclusions:** We identified diverse X chromosomal rearrangements in four haemophilia B patients, which might be caused by distinct mechanisms of genomic rearrangement.

Keywords: chromosomal rearrangement, entire *F9* deletion, haemophilia B, inverse PCR, mapping PCR, MLPA

Introduction

Coagulation factor IX (FIX) is a vitamin K-dependent serine protease and plays an important role in blood coagulation. Haemophilia B is an X-linked recessive bleeding disorder caused by quantitative or qualitative deficiency of FIX, resulting from various defects of the FIX gene (*F9*). Human *F9* contains eight exons and spans 33.5 kb and is located at the distal end of the long arm of the X chromosome (Xq27.1) [1,2]. Based on plasma FIX activity, haemophilia B is classified as severe (<1%), moderate (1–5%) and mild (5–40%) [3], and the phenotypic severity appears to be related to the type and position of the mutations [4]. The FIX Mutation Database has currently reported that a single-point mutation was the gene defect in the vast majority of haemophilia B patients (72.9%); the next most common defect was a gene deletion (16.3%). A deletion of the entire *F9* was reported in 60 haemophilia B cases, including eight Japanese patients. Population-based studies have indicated that 1.5–3% of haemophilia B patients developed inhibitory antibodies in response to treatment products such as plasma-derived or recombinant FIXs [5]. The risk of developing such inhibitor antibodies could increase to >20% in patients with complete deletions of *F9* [6]. Therefore, not only assessment of plasma FIX activity to define the phenotypic severity, but also identification of the type of mutation to assess the risk of inhibitor development, would be usuful for care of haemophilia B patients.

Correspondence: Tetsuhito Kojima, MD, PhD, Professor, Department of Pathophysiological Laboratory Sciences, Nagoya University Graduate School of Medicine, 1-1-20 Daiko-Minami, Higashi-ku, Nagoya 461-8673, Japan.
Tel.: +81 52 719 3153; fax: +81 52 719 3153;
e-mail: kojima@met.nagouya-u.ac.jp

Accepted after revision 14 September 2015

Recently, some haemophilia B cases with entire *F9* deletion have been analysed, and the precise deleted regions of the X chromosome have been identified [7,8]. In these cases, the patients were shown to have lost several functional genes on the X chromosome and showed only bleeding as a symptom, except for a patient with a 4.4-Mb deletion who showed complex clinical symptoms such as hypopituitarism, seizures, severe scoliosis and cognitive delay. In this study, we found four Japanese haemophilia B patients who carried entire *F9* deletions and conducted further analysis to identify the precise genetic abnormalities in their X chromosomes.

Materials and methods

Patients and DNA samples

All subjects were male Japanese patients diagnosed with severe haemophilia B (Table 1). Patients 1, 2 and 4 developed FIX inhibitors, although the inhibitor of Patient 2 disappeared after immune tolerance induction therapy. Patient 4 developed seizures and cognitive delay. The study was approved by the institutional committee for research ethics. After written informed consent was obtained from the patients or parents, genomic DNA samples were isolated from peripheral blood leucocytes by established methods [9].

PCR amplification and MLPA analysis for F9

We amplified all *F9* exons and intron–exon junctions by polymerase chain reaction (PCR) using gene-specific primers for 30 cycles with KOD FX DNA polymerase (Toyobo Co., Ltd., Osaka, Japan) as previously described [10]. The sizes of amplified products were confirmed by electropherogram with a 1.5% agarose gel.

To analyse intragenic deletions or duplications in all four patients, multiplex ligation-dependent probe amplification (MLPA) analysis of *F9* was performed using the SALSA MLPA probemix P207-C2 F9 (MRC-Holland, Amsterdam, The Netherlands) according to the manufacturer's instructions [11].

PCR mapping and identification of deletion breakpoints in X chromosomes

To assess the extent of each deletion, we designed primer pairs for PCR mapping to amplify *F9* fragments in the NCBI reference sequence (NC_000023.11) along both sides of *F9* in chromosome X (Table 2). PCR reactions were performed using KOD FX DNA polymerase at an annealing temperature of 60–66°C, and products were analysed on a 1.5% agarose gel. All the patients are male, and therefore have only one X chromosome; thus we were able to assess the deletion by the absence of PCR products which can be amplified from normal male.

After deleted regions were estimated from the data of mapping PCRs, we amplified the specific DNA sequences over the breakpoints by inverse PCR as described previously [12] or long-range PCR using a specific primer set (Table 2). In brief, for inverse PCR, we digested DNA with the appropriate restriction enzyme (*Eco*RI for Patient 1, *Hin*fI for Patient 2 and *Eco*RV for Patient 3) (New England Biolabs Japan, Inc., Tokyo, Japan), circularized using Ligation high ver.2 (Toyobo Co., Ltd.) and recovered in 5 μL of TE buffer after ethanol precipitation. Each PCR was performed in reactions containing 5 μL of circularized DNA in the presence of 0.5 μM of each primer, 0.4 U of KOD FX DNA polymerase and additional standard PCR reagents in a total volume of 20 μL. Direct

Table 1. Clinical information of haemophilia B cases.

Patient	FIX activity (%)	Age/Sex	FIX inhibitor
1	<1	22/M	+
2	<1	40/M	+*
3	<1	18/M	–
4†	<1	6/M	+

*Inhibitor disappeared after immune tolerance induction (ITI) therapy.
†Patient has seizures and cognitive delay.

Table 2. PCR primer information.

Primer name	Location*	Distance from *F9*	Usage
Patient 1			
C1_Fw (=*Eco*RI_Fw)/Rv	139,444,715/139,444,997	85 kb	Mapping PCR
C2_Fw/Rv	139,446,832/139,447,117	83.6 kb	
T1_Fw/Rv	139,590,171/139,590,630	25 kb	
T2_Fw/Rv	139,610,734/139,611,154	50 kb	
*Eco*RI_Fw (=C1_Fw)/ *Eco*RI_Rv	139,444,715/139,444,466	–	Inverse PCR
Patient 2			
C3_Fw/Rv	139,442,010/139,442,384	88.5 kb	Mapping
C1_ Fw/Rv	139,444,715/139,444,997	85 kb	PCR
T3_Fw/Rv	139,703,998/139,704,388	138 kb	
T4_Fw/Rv	139,728,181/139,728,565	162.5 kb	
*Hin*fI_Fw/Rv	139,442,425/139,442,024	–	Inverse PCR
P2_Fw/Rv	139,442,428/139,715,826	–	Long-range PCR
Patient 3			
C4_Fw/Rv	139,232,218/139,232,655	298 kb	Mapping
C5 _Fw/Rv	139,245,108/139,245,500	285 kb	PCR
T5_Fw/Rv (Patient-3_Rv)	140,420,612/140,421,007	855 kb	
T6_Fw/Rv	140,422,313/140,422,613	857 kb	
*Eco*RV_Fw/Rv	140,422,428/140,422,415	–	Inverse PCR
Patient-3_Fw/Rv (=T5_Rv)	139,234,127/140,421,007	–	Long-range PCR
Patient 4			
C6_Fw/Rv	138,191,766/138,192,086	1338 kb	Mapping
C7_Fw/Rv	138,193,081/138,193,427	1337 kb	PCR
C8_Fw/Rv	138,195,026/138,195,231	1335 kb	
C9_Fw/Rv	138,198,293/138,198,617	1332 kb	
T7_Fw/Rv	145,459,141/145,459,461	5893 kb	
T8_Fw/Rv	145,461,740/145,462,069	5896 kb	
C6_Fw/C8_Rv	138,191,766/138,195,231	–	Long-range
C10_Fw/T8_Rv	138,202,771/145,462,069	–	PCR

*Reference: NC_000023.11, F9: 139,530,733–139,565,697.

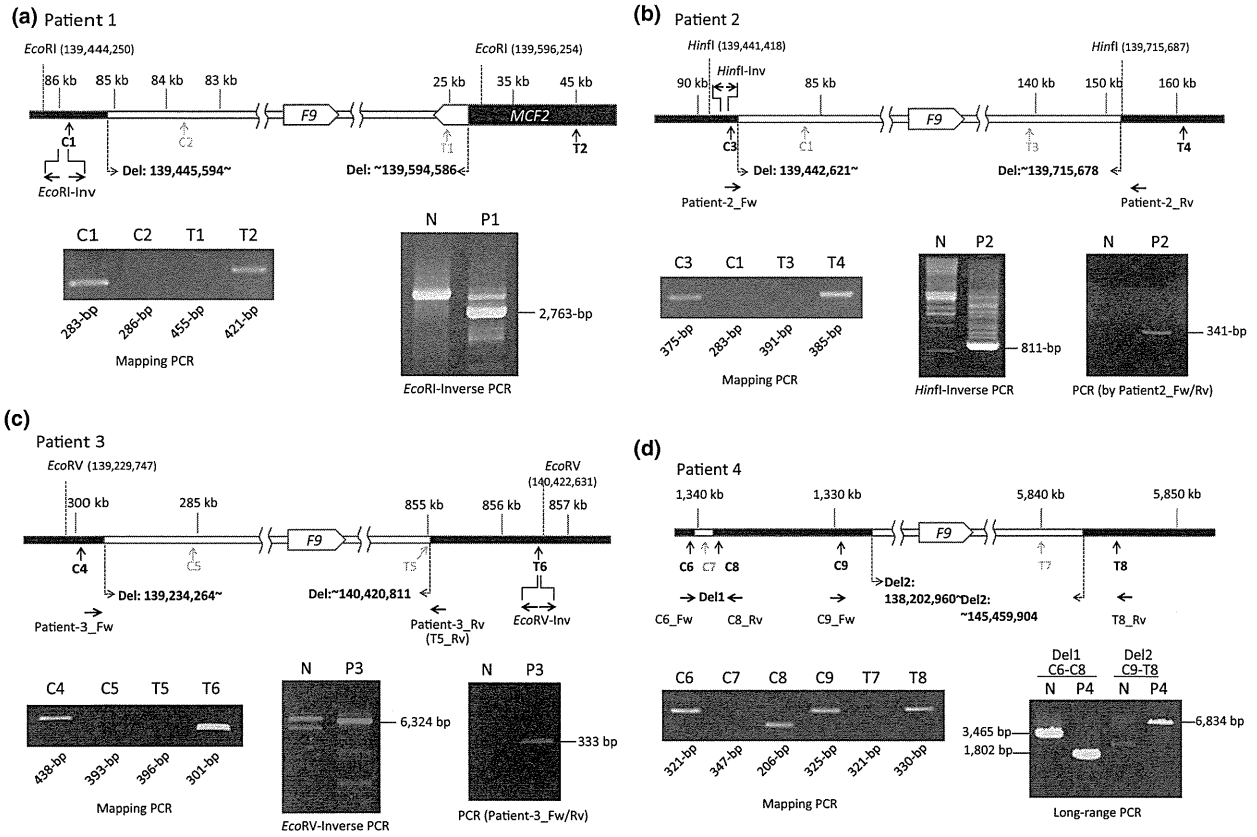

Fig. 1. Schemas of the X chromosomal large deletions and PCRs across the breakpoints in four haemophilia B patients. We performed mapping PCR to assess the extent of the deleted region. We used inverse PCR and/or PCR across the breakpoint followed by direct sequencing to identify the breakpoint. Upward arrows indicate the positions of mapping PCRs. Black and grey symbols indicate success and failure sites of mapping PCRs respectively. N, normal; P1–4, Patient 1–4. (a) Patient 1: Upper panel shows a schema of the X chromosomal large deletion in Patient 1. We identified a 149-kb deletion (g.139,445,594_139,594,586del), including entire *F9* and partial *MCF2*. Lower panel shows results of mapping PCR with respective expected sizes under the photo (left) and *Eco*RI-inverse PCR at the centromere side of the breakpoint in Patient 1 yielding an aberrant 2,763-bp PCR band (right). (b) Patient 2: Upper panel shows a schema of the X chromosomal large deletion in Patient 2. We identified a 273-kb deletion (g.139,442,621_139,715,678del), including entire *F9* and entire *MCF2*. Lower panel shows results of mapping PCR with respective expected sizes under the photo (left), *Hinf*I-inverse PCR at centromere side of the breakpoint in Patient 2 yielding an aberrant 811-bp PCR band (middle), and PCR across the breakpoint yielding a specific 341-bp band (right). (c) Patient 3: Upper panel is a schema of the X chromosomal large deletion in Patient 3, We identified a 1.2-Mb deletion (g.139,234,264_140,420,811del) including *F9*, *MCF2* and *ATP11C*. Lower panel shows results of mapping PCR with respective expected sizes under the photo (left), *Eco*RV-inverse PCR at telomere side of the breakpoint in Patient 3 yielding an aberrant 6,324-bp PCR band (middle), and PCR across the breakpoint yielding a specific 333-bp band (right). (d) Patient 4: Upper panel is a schema of, the X chromosomal large deletion in Patient 4. We identified a 1,663-bp deletion (g.138,192,869_138,194,531del) located 1.34-Mb upstream from *F9* and a 7.26-Mb deletion (g.138,202,960_145,459,904delinsCT) with loss of entire *F9* and other functional genes. Lower panel are results of mapping PCR with respective expected sizes under the photo (left), and PCR across the breakpoints in Patient 4 yielding aberrant 1,802-bp and 6,834-bp bands respectively (right).

sequencing analysis was conducted using the Big Dye Terminator v1.1 Cycle Sequencing kit (Applied Biosystems, Foster City, CA, USA) and the ABI PRISM 310 DNA sequencer; they were performed as previously described [13]. We also performed PCRs to confirm individual sequences of the breakpoint junctions, using specific primers based on the obtained sequence data (Table 2, Table S1).

Results

In the PCR analysis of *F9* abnormality in Japanese haemophilia B patients, we could not obtain any *F9*-specific PCR products from the four subjects, suggesting that they have entire *F9* deletions. The results of MLPA analysis confirmed the complete *F9* deletion in all four patients with absence of peaks for probes targeted to all exons of *F9*. As controls, *F8* and *F7* were examined and revealed that the relative gene dosage values in all exons were 80–120% of normal (Figure S1).

We further analysed the precise deleted regions by mapping PCRs, inverse PCRs and direct sequencing. In Patient 1, a mapping PCR with a primer pair of C1 amplified an amplicon with the correct size but that of C2 did not; this suggests that the centromeric breakpoint was located between C1 and C2 (Fig. 1a). Furthermore, we performed an *Eco*RI-inverse PCR at the centromere side of the breakpoint (*Eco*RI sites;

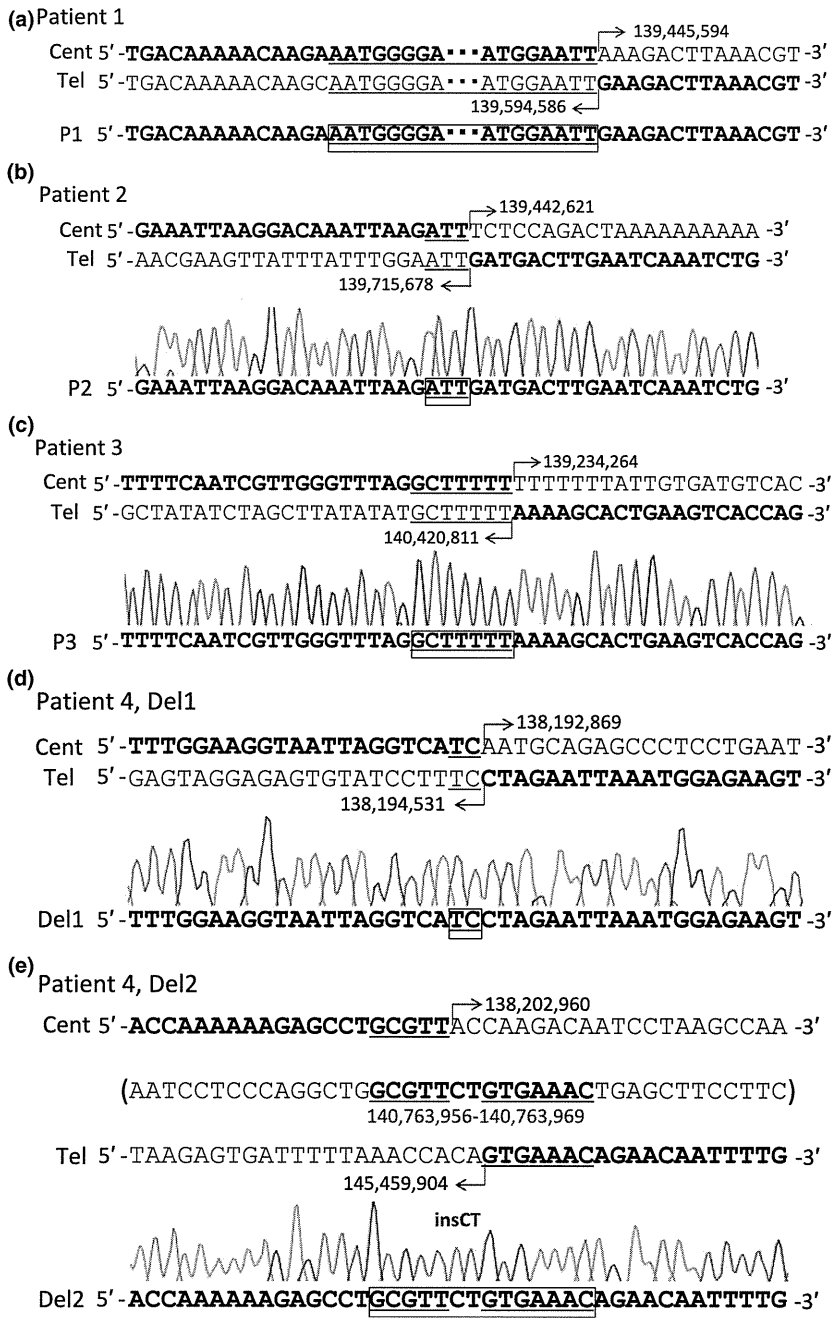

Fig. 2. DNA sequences over the breakpoints. (a) Patient 1 (g.139,445,594_139,594,586 del). A part of LINE-1 sequence was observed at the junction. (b) Patient 2 (g.139,445,594_139,594,586 del). A 3-bp homologous sequence (ATT) was observed at the junction. (c) Patient 3 (g.139,234,264_140,420,811 del). A 7-bp homologous sequence (GCTTTTT) was observed at the junction. (d) Patient 4, Del1 (centromeric deletion: g.138,192,869_138,194,531del). A 2-bp homologous sequence (TC) was observed at the junction. (e) Patient 4, Del2 (telomeric deletion: g.138,202,960_145,459,904delinsCT). A 2-bp insertion was observed at the breakpoint (delinsCT). A 14-bp sequence in parentheses, including inserted CT corresponding to the breakpoint, was found at 2.56-Mb on the centromere side of the breakpoint. Cent, sequences around centromeric breakpoint; Tel. sequences around telomeric breakpoint; bold type sequences, not deleted sequences; under line, homologous sequences; boxed sequences, homologous sequences at the junctions.

139,444,250 and 139,596,254) using a primer set (*Eco*RI_Fw/Rv in Table 2) and obtained a specific 2763-bp PCR product (Fig. 1a). Direct sequencing of the inverse PCR product revealed a 149-kb deletion (g.139,445,594_139,594,586del), including the entire *F9* gene and a partial deletion of *MCF2* (Fig. 2a). The breakpoint was located 85-kb upstream and 30-kb downstream from *F9*. Centromeric and teromeric genomic DNAs of the breakpoint possessed approximately 120 bp of identical sequence, which is a part of the long interspersed nucleotide element-1 (LINE-1).

Similarly, in Patient 2, a mapping PCR with a primer pair of C3 amplified an amplicon with the correct size, but the C1 primers did not (Fig. 1b). Direct sequencing of a *Hin*fI-inverse PCR product at the centromere side of the breakpoint using a primer set (*Hin*fI_Fw/Rv in Table 2) and that of PCR amplification over the breakpoint using a primer pair of patient-2_Fw/Rv revealed a 3-bp homologous sequence consisting of ATT at the centromeric and teromeric breakpoint junctions. Thus, Patient 2 showed a 273-kb deletion (g.139,442,621_139,715,678del), including entire *F9* and entire *MCF2* (Fig. 2b).

Table 3. Information for gene deletions.

Case	Extent	Region (Ref: NC_000023.11)	Deleted genes
1	148 993 bp (149 kb)	g.139,445,594_139,594,586del	*F9*, *MCF2* (partial)
2	273 058 bp (273 kb)	g.139,442,621_139,715,678del	*F9*, *MCF2*
3	1 186 548 bp (1.19 Mb)	g.139,234,264_140,420,811del	*F9*, *MCF2*, *ATP11C*
4	1663 bp	g.138,192,869_138,194,531del	*FGF13*, *F9*, *MCF2*, *ATP11C*, *SOX3*, *CDR1*,
	7 256 945 bp (7.26 Mb)	g.138,202,960_145,459,904delinsCT	*SPANXB1*, *LDOC1*, *SPANXC*, *SPANXA1,2*, *MAGEC3*, *MAGEC1*, *MAGEC2*, *SPANXN3*, *SLITRK4*, *SPANXN2*, *USBE2NL*, *SPANXN1*

In Patient 3, a mapping PCR with a primer pair of T6 amplified an amplicon with the correct size but the T5 primers did not (Fig. 1c). We conducted an *Eco*RV-inverse PCR at the telomere side (*Eco*RV site; 139,229,747 and 140,422,631) using a primer set (*Eco*RV_Fw/Rv in Table 2). Direct sequencing of an *Eco*RV-inverse PCR product (6324-bp) by primer walking at the telomere side and that of a PCR amplification (333-bp) over the breakpoint by patient-3_Fw/Rv revealed a 1.2-Mb deletion (g.139,234,264_140,420,811del), including *F9*, *MCF2* and *ATP11C* (Figs 1c and 2c) and a 7-bp homologous sequence (GCTTTTT) at the junction.

In Patient 4, a mapping PCR showed two deleted regions in the X chromosome (Fig. 1d). In addition, we conducted long-range PCRs by C6_Fw/C8_Rv and C9 Fw/T8_Rv, resulting in the amplification of specific bands (1802-bp and 6834-bp respectively). Direct sequencing of the PCR products revealed a 1663-bp deletion (g.138,192,869_138,194,531del) located 1.34-Mb upstream from *F9* with a 2-bp homologous sequence (TC) at the junction (Fig. 2d) and a 7.26-Mb deletion (g.138,202,960_145,459,904delinsCT) with the loss of entire *F9* and other functional genes (Fig. 2e, Table 3). The latter large-scale deletion had no homologous sequence, but a 2-bp insertion was observed at the breakpoint (delinsCT). The 14-bp sequence including this inserted CT corresponding to the breakpoint was found at 2.56-Mb on the centromere side of the breakpoint (g.140,763,965_140,763,969).

Discussion

We detected entire *F9* deletions in four Japanese haemophilia B patients by MLPA and identified diverse deleted regions in their X chromosomes. Currently, the entire deletion of *F9* has been reported in 12 haemophilia B patients in Japan, including the four cases in this study. In general, large deletions, nonsense mutations and splicing defects of *F9* in haemophilia B patients are high risks factor for developing FIX inhibitors. In this study, patients 1, 2 and 4 had developed a FIX inhibitor. Patient 3 was appeared to lack a FIX inhibitor at this moment, and such cases should be paid close attention to with regards to the development of FIX inhibitor in future.

In patients 1 and 2, we found partial or entire deletion of *MCF2* (a member of a large family of GDP–GTP exchange factors). Previously, two unrelated haemophilia B patients who had a deletion, including *F9* and *MCF2*, were reported to have no clinical symptoms attributed to the loss of *MCF2* [14].

Patient 3 lost *ATP11C* (ATPase, class VI, type 11C), which displays flippase activity. In patient 4, the deleted region contains *F9* and 19 other genes, including *FGF13*, *MCF2*, *ATP11C*, *SOX3*, *LDOC1* and others, and their functions are still unclear. *ATP11C* and *LDOC1* (Leucine zipper, Downregulated in cancer 1) are associated with B-cell development. *FGF13* (Fibroblast growth factor 13) is a candidate gene for syndromal and non-specific forms of X chromosome-linked mental retardation (XLMR). Wu *et al.* showed that FGF13 is a microtubule-stabilizing protein, regulating neural polarization and migration in the cerebral cortex [15]. In their study, the loss of *FGF13* in mice results in neuronal migration defects in both the neocortex and the hippocampus, with associated weakened learning and memory. Sex determining region Y-box 3 (*SOX3*) is an early developmental transcription factor involved in pituitary development [16]. In humans, over- or under-dosage of *SOX3* is associated with X-linked hypopituitarism, with variable phenotypes ranging from isolated growth hormone deficiency to pan hypopituitarism with or without mental retardation; in addition, it has been associated with an ectopic/undescended posterior pituitary in most cases with reported pituitary imaging.

Recently, seven cases with large deletions in *F9*, including four entire *F9* deletions were reported [7]. These four patients only exhibited bleeding without other clinical manifestations, although some had partial loss of *FGF13*, partial or entire loss of *MCF2* and complete loss of *ATP11C*. Another haemophilia B patient with a large deletion similar to that in patient 4 was reported [8] who had a 4.4-Mb deletion (g.138,398,378_142,801,670del), including *FGF13*, *F9*, *MCF2*, *ATP11C*, *SOX3* and *LDOC1*. The patient showed other complex clinical symptoms, consisting of hypopituitarism, seizures, severe scoliosis and cognitive delay. In patient 4 in our study, seizures and cognitive delay were also observed, which is likely to be predominantly caused by the loss of *SOX3*.

Previously, genomic rearrangements were described as gross DNA changes because of duplication, deletion, insertion or inversion, ranging from thousands to sometimes millions of base pairs. Some major mechanisms have been proposed for genomic rearrangements in the human genome: non-allelic homologous recombination (NAHR), non-homologous end joining (NHEJ) and Fork Stalling and Template Switching/microhomology-mediated break-induced replication (FoSTeS/MMBIR) models [17–23]. NAHR leads to genomic rearrangements between two low-copy repeats or repetitive sequences such as LINE and Alu elements [18]. Therefore, the mechanism of deletion caused between two LINE 1 elements in patient 1 may be NAHR. NHEJ is one of the double-stranded DNA break (DSB) repair mechanisms; it proceeds by the interaction of broken DNA ends without homology or with a few homologous sequences [17,19]. In this model, extra nucleotides are often found at the junction of genomic rearrangements [20]. FoSTeS/MMBIR models are proposed as the mechanisms to explain complex deletion and duplication rearrangements instead of NAHR or NHEJ [21–23]. FoSTeS is a DNA replication-based model, which occurs during mitosis, and MMBIR is based on the BIR repair mechanism, which associates a repair of single-end DSB. However, genomic rearrangements by FoSTeS/MMBIR occur via DNA interactions using microhomologies.

At the breakpoints in patients 2 and 3 and the shorter deletion in patient 4, microhomologies ranging from 2 to 7 bp were detected; therefore, these deletions could result from NHEJ or FoSTeS/MMBIR. The larger deletion in patient 4 had a 2-bp insertion at the breakpoint but no microhomology at the breakpoint, which appeared to be a genomic rearrangement caused by NHEJ with extra nucleotides. However, in this case, a 14-bp sequence, including a CT insertion over the breakpoint, was found in the middle of the deleted region with 5- and 7-bp microhomology at centromere and telomere breakpoints respectively. Therefore, FosTes/MMBIR may explain the mechanism of this extensive deletion.

Wu *et al.* suggested that NHEJ and MMBIR may be the major mechanisms accounting for the large *F9* deletion [7]. They reported that only one patient had a deletion between two LINE 1 elements caused by NAHR, and deletions associated with NHEJ or MMBIR accounted for six out of seven cases. In our study, NHEJ or FoSTeS/MMBIR is the mechanism responsible for majority of the large deletions and the deletions that include the entire *F9*.

In conclusion, we used MLPA to detect entire *F9* deletions in four Japanese haemophilia B patients and identified diverse deleted regions in their X chromosomes, which may be caused by distinct mechanisms of genomic rearrangement, such as NHEJ, NAHR or FoSTeS/MMBIR. A severe haemophilia B patient with seizures and cognitive delay was found to have lost several functional genes, including entire *F9* and *SOX3*, indicating that co-deletion of these two genes can cause complex clinical symptoms.

Acknowledgements

The authors thank Ms. C Wakamatsu for her expert technical assistance, Ms. M. Goto for data collection and Drs M. Yamamoto, S. Hanabusa and M. Ishimura for patient enrolment. This study was financially supported in part by the Ministry of Health, Labour and Welfare Research Subsidy Program (TK and MS). The authors also thank Enago for review of the English language.

Author contributions

YN performed the research and drafted the manuscript; YA, YT, MM, TK, YN, RH and AT performed the research and contributed to the analytic methodology; TM and MS collected the clinical samples and T. Kojima designed the research study and wrote the manuscript. All authors were involved in critical reading of the manuscript prior to submission.

Disclosures

The authors stated that they had no interests which might be perceived as posing a conflict or bias.

References

1 Anson DS, Choo KH, Rees DJ *et al.* The gene structure of human anti-haemophilic factor IX. *EMBO J* 1984; **3**: 1053–60.
2 Yoshitake S, Schach BG, Foster DC, Davie EW, Kurachi K. Nucleotide sequence of the gene for human factor IX (antihemophilic factor B). *Biochemistry* 1985; **24**: 3736–50.
3 White GC, Rosendaal F, Aledort LM *et al.* Definitions in hemophilia. Recommendation of the scientific subcommittee on factor VIII and factor IX of the scientific and standardization committee of the International Society on Thrombosis and Haemostasis. *Thromb Haemost* 2001; **85**: 560.
4 Lillicrap D. The molecular basis of haemophilia B. *Haemophilia* 1998; **4**: 350–7.
5 Warrier I, Lusher JM. Development of anaphylactic shock in haemophilia B patients with inhibitors. *Blood Coagul Fibrinolysis* 1998; **9**(Suppl 1): S125–8.
6 Thorland EC, Drost JB, Lusher JM *et al.* Anaphylactic response to factor IX replacement therapy in haemophilia B patients: complete gene deletions confer the highest risk. *Haemophilia* 1999; **5**: 101–5.
7 Wu X, Lu Y, Ding Q *et al.* Characterisation of large F9 deletions in seven unrelated patients with severe haemophilia B. *Thromb Haemost* 2014; **112**: 459–65.
8 Hewitt J, Chou EM, Brown LA *et al.* Molecular characterization of a 4,409,480 bp deletion of the human X chromosome in a patient with haemophilia B. *Haemophilia* 2014; **20**: e230–4.
9 Kojima T, Tanimoto M, Kamiya T *et al.* Possible absence of common polymorphisms in coagulation factor IX gene in Japanese subjects. *Blood* 1987; **69**: 349–52.
10 Okumura K, Fujimori Y, Takagi A *et al.* Skewed X chromosome inactivation in fraternal female twins results in moderately severe and mild haemophilia B. *Haemophilia* 2008; **14**: 1088–93.
11 Kwon MJ, Yoo KY, Kim HJ, Kim SH. Identification of mutations in the F9 gene including exon deletion by multiplex ligation-dependent probe amplification in 33

unrelated Korean patients with haemophilia B. *Haemophilia* 2008; **14**: 1069–75.
12 Fujita J, Miyawaki Y, Suzuki A *et al.* A possible mechanism for Inv22-related F8 large deletions in severe hemophilia A patients with high responding factor VIII inhibitors. *J Thromb Haemost* 2012; **10**: 2099–107.
13 Tsukahara A, Yamada T, Takagi A *et al.* Compound heterozygosity for two novel mutations in a severe factor XI deficiency. *Am J Hematol* 2003; **73**: 279–84.
14 Anson DS, Blake DJ, Winship PR, Birnbaum D, Brownlee GG. Nullisomic deletion of the mcf.2 transforming gene in two haemophilia B patients. *EMBO J* 1988; **7**: 2795–9.
15 Wu QF, Yang L, Li S *et al.* Fibroblast growth factor 13 is a microtubule-stabilizing protein regulating neuronal polarization and migration. *Cell* 2012; **149**: 1549–64.
16 Alatzoglou K, Azriyanti A, Rogers N *et al.* SOX3 deletion in mouse and human is associated with persistence of the craniopharyngeal canal. *J Clin Endocrinol Metab* 2014; **99**: E2702–8.
17 Gu W, Zhang F, Lupski JR. Mechanisms for human genomic rearrangements. *Pathogenetics* 2008; **1**: 4.
18 Shaw CJ, Lupski JR. Implications of human genome architecture for rearrangement-based disorders: the genomic basis of disease. *Hum Mol Genet* 2004; **1** Spec No 1: R57–64.
19 Lieber MR. The mechanism of human nonhomologous DNA end joining. *J Biol Chem* 2008; **283**: 1–5.
20 Roth DB, Chang XB, Wilson JH. Comparison of filler DNA at immune, nonimmune, and oncogenic rearrangements suggests multiple mechanisms of formation. *Mol Cell Biol* 1989; **9**: 3049–57.
21 Lee JA, Carvalho CM, Lupski JR. A DNA replication mechanism for generating nonrecurrent rearrangements associated with genomic disorders. *Cell* 2007; **131**: 1235–47.
22 Hastings PJ, Ira G, Lupski JR. A microhomology-mediated break-induced replication model for the origin of human copy number variation. *PLoS Genet* 2009; **5**: e1000327.
23 Sakofsky CJ, Ayyar S, Malkova A. Break-induced replication and genome stability. *Biomolecules* 2012; **2**: 483–504.

Supporting Information

Additional Supporting Information may be found in the online version of this article:

Figure S1. MLPA analysis data.

Table S1. PCR primer sequences.

第76回日本血液学会学術集会
Symposium 9
The front line of thrombosis and hemostasis research

アンチトロンビンレジスタンス ―新しい遺伝性血栓性素因―

小嶋哲人，　高木　明，　村田　萌，　高木夕希

静脈血栓塞栓症は様々な先天的/後天的リスクにより発症する多因性疾患で，従来欧米人に多く日本人には少ないとされてきたが，診断技術の向上や食生活の欧米化などにより日本人にも決して少なくないことが明らかにされている。遺伝性血栓症の原因として様々な凝固関連因子の遺伝子異常が同定されているが，いまだに原因不明な遺伝性血栓症もある。我々は長らく原因不明であった遺伝性静脈血栓症家系において，通常は出血症状を示すプロトロンビン異常症で逆に血栓症の原因となる遺伝子変異を発見した。詳細な解析結果から，この変異由来トロンビンは凝固活性がやや弱いものの，アンチトロンビン（AT）による不活化に抵抗性を示すため長時間活性が残存するため血栓症の原因となることが判明し，新しい血栓性素因・ATレジスタンス（ATR）として報告した。本稿では，新しい遺伝性血栓性素因・ATRについて最近の知見も踏まえて概説する。（臨床血液56（6）：632～638，2015）

Key words : Hereditary thrombophilia, Prothrombin Yukuhashi, Antithrombin resistance

はじめに

静脈血栓塞栓症（venous thromboembolism, VTE）は，深部静脈血栓症（deep vein thrombosis, DVT）と肺血栓塞栓症（pulmonary embolism, PE）を合わせた疾患概念で，遺伝的リスクと環境的リスクの発症要因が重なり発症する[1]。VTEは，欧米人に比べ日本人には少ないとされてきたが，診断技術の向上や食生活の欧米化などのため日本人においても決して少なくないことが明らかになっている。VTE発症の遺伝的リスクには，アンチトロンビン（antithrombin, AT）やプロテインC（protein C, PC），プロテインS（protein S, PS）などの生理的血液凝固阻止因子の遺伝子異常に伴う先天性欠乏症/異常症が広く知られ，欧米人と同様に日本人においても数多くの遺伝子異常が報告されている。特に，PS Tokushima変異（p.K196E）は一般日本人でも55人に1人の頻度でヘテロが存在することが報告され[2]，日本人特有の血栓性素因であることが明らかとなっている。一方，VTE発症患者の同一家系内でも，同じ遺伝子異常をもちながら症候性VTEを発症しない同胞もしばしばみられ，多因性疾患であるVTEの発症には遺伝子的リスクに加えて環境的リスクなどで複数のリスクの重複がその発症率を増大させているものと考えられる。

日本人のVTE発症患者のうち，遺伝子変異を同定できる割合はおよそ3割とされ，明らかに遺伝性が疑われる症例でも未だに原因不明の遺伝性血栓症が数多くある。こうした中で我々は，長らく原因不明であった静脈血栓症の多発する家系において，通常では出血症状が問題となるプロトロンビン異常症で逆に血栓症の原因となる遺伝子異常を発見し，新しい血栓性素因・アンチトロンビンレジスタンス（AT resistance, ATR）として報告した[3,4]。本稿では，この新しい先天性血栓性素因・ATRと血漿検体を用いてのATR検出検査法の開発について，最近の知見も踏まえて概説する。

1．先天性血栓性素因

血管損傷時には，生体防御機構の一つとしてその局所ですみやかに血栓形成による止血機構が働き出血を防いでいる。一方で，健常血管壁においては通常では血栓が生ずることないように，また止血血栓形成が過剰に進行しないように，生理的な血液凝固の抑制機構が働いている。生体防御反応である止血血栓形成は，血管内皮，血小板，凝固線溶因子ならびにそれらの阻止因子などによる巧妙な連携制御のもとに営まれているが，何らかの異常に伴いこれらの連携制御のバランスが崩れると病的な血栓症や出血症状が生じてしまうことになる。病的血栓症の原因となる遺伝的リスクとしての先天性血栓性素因

名古屋大学大学院医学系研究科　病態解析学講座

には，凝固反応抑制に問題が生ずる「凝固阻止因子の遺伝子異常」と過剰な凝固反応をもたらす「凝固因子の遺伝子異常」が知られている。

生理的凝固阻止因子の遺伝子である *SERPNC1*（AT），*PROC*（PC），*PROS1*（PS）の異常には，それぞれの欠乏症/異常症による血栓性素因となる変異が報告されており[5~7]，日本人の静脈血栓症患者からも数多くの遺伝子変異が同定されている[8]。なかでも，PS p.K196E 変異（PS Tokushima）は日本人特有の先天性血栓性素因として知られ，日本人の 55 人に 1 人がヘテロ接合体として変異を保有すると報告されている[2]。

欧米人に多い遺伝的リスクとして，活性化 PC レジスタンス（APC resistance）を示す凝固第 V 因子（FV）R506Q 変異（FV Leiden）[9]や，プロトロンビン遺伝子の 3' 非翻訳領域変異により血漿中プロトロンビン濃度が上昇するプロトロンビン G20210A 変異[10]が有名である。しかし，これらは日本人をはじめ東アジア人には報告がなく，欧米人に血栓症が多い要因の一つとされている。また，ごく希な報告としては，凝固第 IX 因子（FIX）遺伝子異常が出血性素因（血友病 B）ではなく，逆に FIX 活性が異常高値（700%）を示す遺伝性血栓症の原因となる FIX Padua 変異がある[11]。

2. 新たな先天性血栓性素因・アンチトロンビンレジスタンス（ATR）

我々は，長らく原因が特定できなかった静脈血栓症家系において，通常，出血傾向となるプロトロンビン異常症で逆に血栓症の原因となる遺伝子異常を同定し，新しい血栓性素因・アンチトロンビンレジスタンス（ATR）として報告した[3,4]。これは，FV Leiden が同様に凝固因子のミスセンス変異でありながら凝固活性は保たれ，かつその凝固活性は活性化 PC（APC）による不活化に抵抗性を示すため，結果として血栓傾向となる病態と似ている[9]。

1）プロトロンビン Yukuhashi 変異の発見

発端者は 3 世代にわたり静脈血栓症が多発する日本人家系に生まれた女性で，11 歳時に DVT を発症し，2001 年当時に既知の先天性血栓性素因について調査がされたが，異常は検出されなかった[12]。2009 年にボストンで開催された国際血栓止血学会（ISTH）において，ある遺伝性血栓症家系のゲノムワイド連鎖解析からプロトロンビン遺伝子異常の存在が報告された[13]。その報告を受けて我々が発端者の解析を行ったところ，プロトロンビン遺伝子にミスセンス変異・プロトロンビン Yukuhashi 変異（c.1787G>T, p.R596L）を同定した（Fig. 1）。

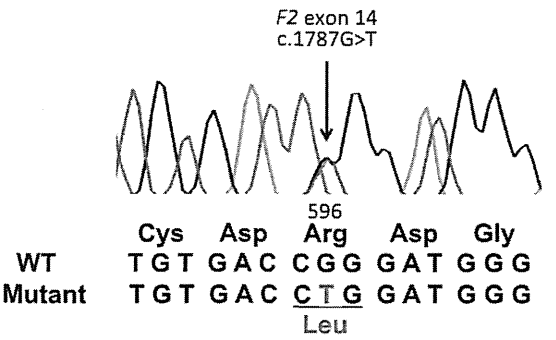

Fig. 1 Prothrombin gene (*F2*) mutation conveying antithrombin resistance (modified from ref. 3.)
A missense mutation (c.1787G> A, p.R596L) located at the AT binding site of thrombin was identified.

2）プロトロンビン Yukuhashi 変異による血栓症発症機序

プロトロンビンのアルギニン（R596）は，活性化されたトロンビンが AT と複合体（TAT）を形成して不活化される際に，AT のアスパラギン（N265）と水素結合を形成することが報告されている[14]。したがって，プロトロンビン Yukuhashi 変異（c.1787G>T）による R596L 置換はトロンビンへと活性化された後の AT による不活化不全を起こすことが予想されたこと，この R596L 置換変異が患者ならびに家系内の血栓症患者にも検出されたことから，本家系での遺伝性血栓症の原因であることが強く疑われた。患者はすでにワルファリン治療を受けているため，患者由来の変異プロトロンビンの機能解析は正しく評価できないため，我々は遺伝子工学的技法を用いて野生型/変異型プロトロンビンをリコンビナント蛋白として HEK29 細胞内で合成させ，そのトロンビンへの活性化動態，活性化後の AT による不活化動態を比較検討した。

3）Yukuhashi 変異プロトロンビンのトロンビンへの活性化

変異型プロトロンビンの機能解析のため，プロトロンビン欠乏血漿にそれぞれ野生型あるいは変異型リコンビナントプロトロンビンを添加して疑似血漿を作製し，凝固一段法，凝固二段法，および合成基質（S-2238）法の 3 つの方法で野生型/変異型プロトロンビンの活性を測定した。その結果，野生型はいずれの測定法でも正常血漿とほぼ同当な数値を示したが，変異型では 3 つ全ての方法で野生型を下回り，凝固一段法で最も低く（15%），次いで凝固二段法（32%），蛍光基質法（66%）の順で数値が大きくなった。すなわち，変異型プロトロンビンはトロンビンへの活性化がやや遅延し，フィブリノゲンを基質とした活性も低下すること，フィブリノゲンに比

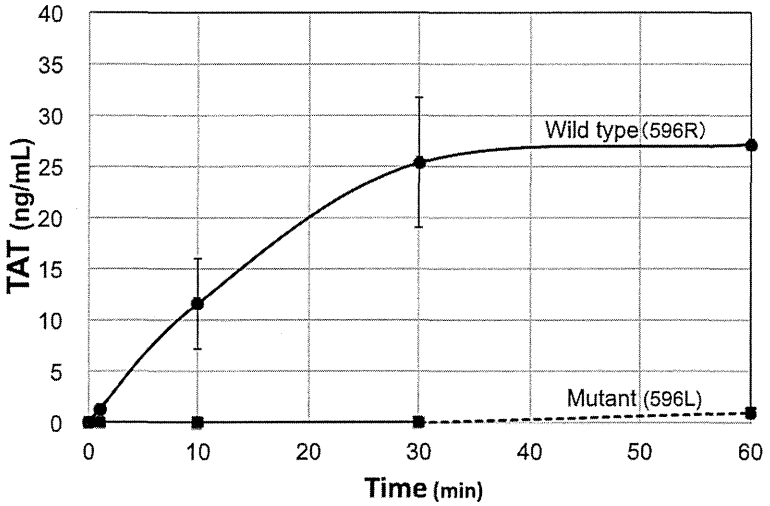

Fig. 2 Thrombin-antithrombin (TAT) complex formation (modified from ref. 3.)
After conversion of recombinant prothrombins (Wild type, 596R; Mutant, 596L) to thrombins and addition of antithrombin (AT), thrombin-AT (TAT) complex formation was measured by ELISA. Compared to the wild type, the mutant formed very little amounts of TAT.

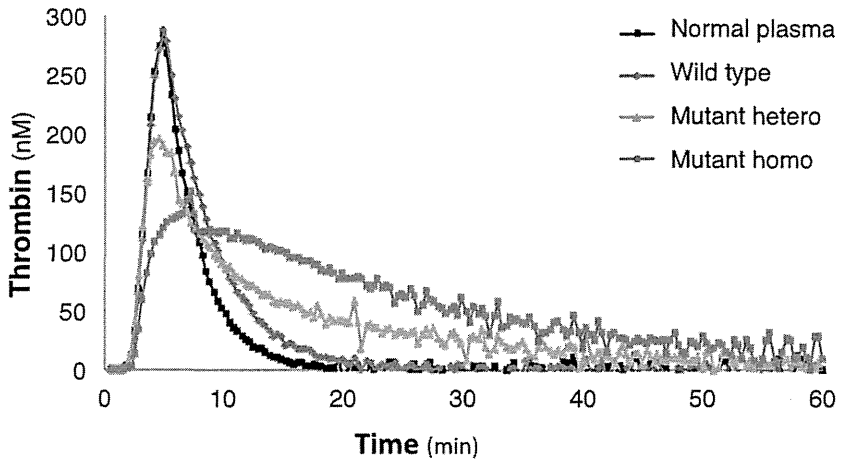

	Normal plasma	Wild type	Mutant hetero	Mutant homo
ETP (nM.min)	1276	1658	2374	3620
Peak (nM)	284	283	194	144
StartTail (min)	23.5	26.5	78.0	105.0

Fig. 3 Thrombin generation assay (TGA) (modified from ref. 3.)
Results of a thrombin-generation assay of normal plasma and reconstituted plasma samples, with recombinant prothrombins in prothrombin-deficient plasma, were shown. Heterozygous mutant (Mutant hetero) plasma contained 50% each of wild type and mutant prothrombins. Table shows the total amount of thrombin activity (endogenous thrombin potential: ETP), the maximum concentration of thrombin (Peak), and the total duration of thrombin-generation activity (Start tail).

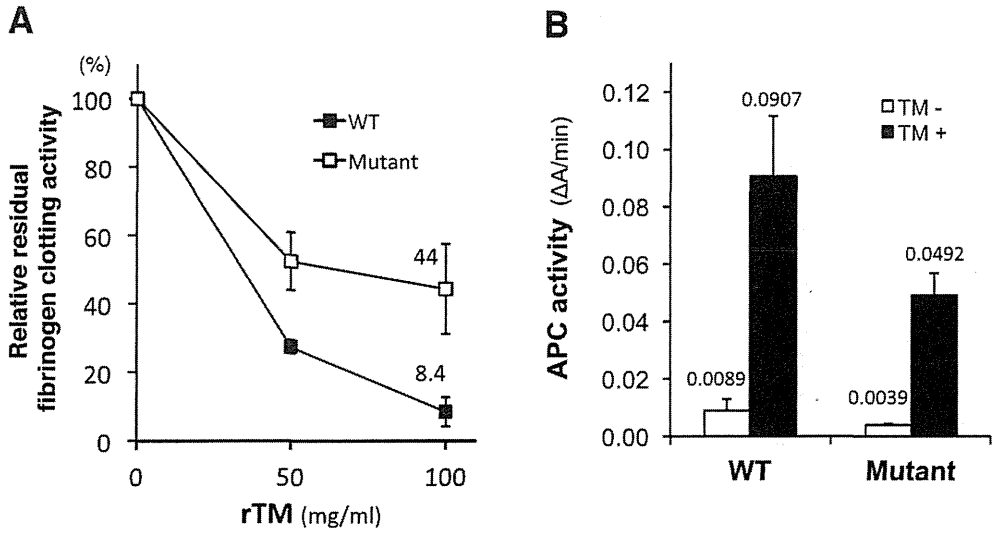

Fig. 4 TM effects on fibrinogen clotting and APC generation activities (modified from ref. 15.)
A: Wild-type and mutant thrombins were incubated with rTM (0, 50, and 100 μg/ml) for a minute, and relative residual fibrinogen-clotting activities were measured.
B: Recombinant prothrombins were sufficiently activated to thrombins using Ox venom, human PC was then added, and the combination was incubated for 60 min in the absence or presence of rTM. After the residual thrombin activity was blocked by Pefabloc-TH, APC activities were measured using S-2366 and expressed as ΔA/min at 405 nm.

べ分子量が小さい合成基質を用いて測定した活性はあまり低下しないことが観察された。

4) Yukuhashi 変異トロンビンの不活化

変異型プロトロンビンをトロンビンへ活性化後，ATとの結合能（トロンビン・AT（TAT）複合体形成能）について野生型と比較検討した。その結果，ヘパリン非存在下では野生型トロンビンでは時間依存的にTAT形成が見られたのに対し，変異型トロンビンはATとの複合体形成がほとんど見られず，ATにより不活化されないことが予想された（Fig. 2）。ヘパリン存在下では変異型，野生型ともに継時的なTAT複合体上昇が見られたが，1分後のTAT複合体形成は野生型の約半分程度にとどまっていた。これらの結果から，患者体内でも変異型異常トロンビンはATによる不活化反応が強く障害されていることが予想された。

一方，プロトロンビン欠乏血漿に変異型/野生型プロトロンビンを50%ずつ添加した疑似患者血漿でのトロンビン生成試験（Thrombin generation assay, TGA）では，野生型プロトロンビンを100%加えた疑似正常血漿や正常プール血漿と比較して，最高トロンビン活性がやや低いものの不活化が著しく遅延し，結果として総トロンビン活性量に相当するETP（Endogenous thrombin potential）の著しい増大を認めた（Fig. 3）。すなわち，患者血漿中の異常プロトロンビンは，血液凝固活性は低いものの一旦活性化されるとATRを示して凝固活性（フィブリン生成能）を保ち続けることが予想され，これが本家系の遺伝性血栓症の原因になることが示唆された。

5) Yukuhashi 変異トロンビンの TM-PC 抗凝固系への影響

トロンビンは多面的な生理活性をもつ蛋白で，抗凝固分子のトロンボモジュリン（TM）と結合するとフィブリン形成能を失い，抗凝固分子であるプロテインC（PC）を活性化することで一転して抗凝固作用を示す。プロトロンビンYukuhashi由来の変異型トロンビンのTM−PC系に及ぼす影響解析した結果，リコンビナント可溶性TM（rTM：旭化成ファーマ株式会社より供与）の存在下では野生型トロンビンの相対的フィブリノゲン凝固活性は用量依存的に8.4%まで低下し，一方で変異型トロンビンは44%までの低下にとどまっていた（Fig. 4A）。また，rTM非存在下において活性化PC（activated protein C, APC）の産生能（ΔA/min［吸光度変化率］at 405nm）はわずか（野生型トロンビンで0.0089，変異型トロンビンで0.0039）であったが，rTMの添加によって野生型で0.0907（10.2倍），変異型で0.0492（12.6倍）まで増強した（Fig. 4B）。これらのデータは，プロトロンビンYukuhashi変異では，TMによるAPC産生増強能は維持されるものの，フィブリノゲン凝固抑制におい

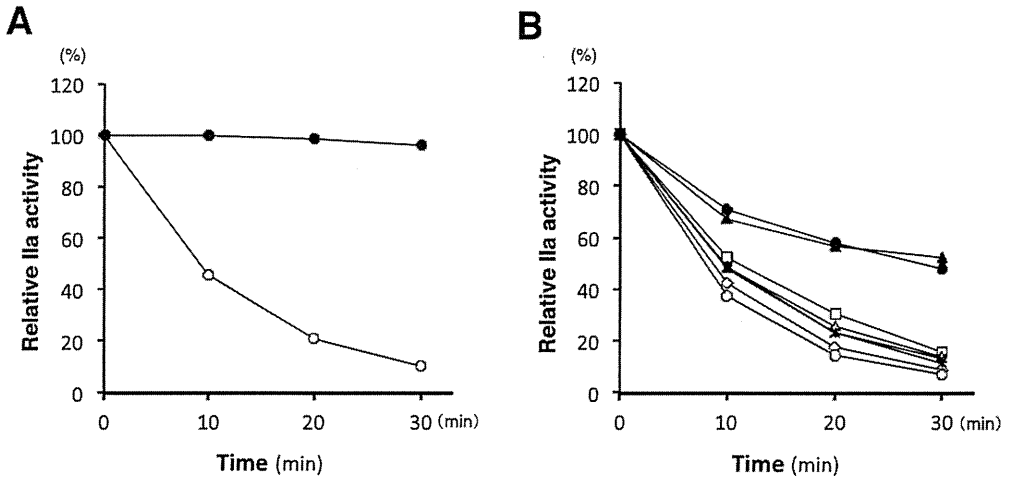

Fig. 5 ATR detecting assay in plasma (modified from ref. 16.)
A: Activated thrombins from recombinant prothrombins were inactivated using AT without heparin for 0–30 min, and relative residual thrombin activities were determined. Relative residual thrombin activities were calculated by comparison with the 0-min data. ○, wild type recombinant prothrombin; ●, mutant recombinant prothrombins. B: Relative residual thrombin activities were determined. There were statistically significant differences between the data of the patients (●, ▲) with and the patients (□, △, ◇, ＊) without the prothrombin Yukuhashi mutation. ○, normal plasma.

てTM抵抗性を示すことでも静脈血栓症を引き起こしやすくなる可能性が示唆された[15]。

6）ATR検出検査法の開発

我々は，ATによるトロンビン不活化動態を合成基質法で解析観察することでATRを検出する臨床検査法を開発した[16]。これは，血漿検体を用いてプロトロンビナーゼ様活性をもつTypan蛇毒（*Oxyuranus scutellatus* (Ox)）によりトロンビンへと活性化した後，ATによる不活化動態を各反応時間での残存トロンビン活性として測定観察するものである。本検査法において，プロトロンビン欠乏血漿に野生型ATを添加した野生型疑似血漿で，血中濃度5倍量ATの添加後30分では約10%にまでトロンビン活性が阻害されたのに対し，変異型ホモ疑似血漿では30分後でも90%以上残存していた（Fig. 5A)。また，静脈血栓症患者でのワルファリン服用中検体を用い，ワルファリンが本測定法に及ぼす影響について検討した結果，考案した検査法はATによるトロンビン活性の不活化動態を相対的に観察するため，ワルファリン服用中の検体であっても解析可能であった。すなわち，ワルファリン服用中のR596L変異をもっていない血栓者患者では30分後にはいずれも20%以下まで残存トロンビン活性が低下したのに対し，2名のR596L変異ヘテロ保有患者血漿のそれはともに約50%の残存トロンビン活性が観察され，ATRであると判定できる（Fig. 5B)。ごく最近，我々はN Engl J Med誌に報告した家系とは異なる日本人静脈血栓症家系において，上述の血漿検体でのATR検出法での解析により新たなATR日本人症例を同定している[17]。

7）ATRを示す新たな変異症例

2013年Djordjevicらは，遺伝性血栓症をもつセルビア人2家系でプロトロンビン遺伝子変異（c.1787G>A, p.Arg596Gln: プロトロンビンBelgrade）を報告したが，我々が開発した検出法ではいずれもATRを示していた[18]。また，同年にインド人血栓症患者においても同じ変異が報告されている[19]。ごく最近，上述のごとく我々は日本人2家系目のATR家系を血漿検体での検出法により同定したが，その遺伝子解析ではセルビア人変異（プロトロンビンBelgrade）と同じc.1787G>A変異を検出し[17]，さらに別家系の日本人血栓症症例でもATRを検出し，やはりc.1787G>A変異を同定している（日本人3家系目)。したがって，血栓性素因・ATRは日本人だけでなく欧米人をはじめ他の人種にも遺伝性血栓症の原因として存在していることが明らかとなった。血漿検体でのATR検出法の普及は，厳密な倫理的配慮が必要な遺伝子解析に比べて利便性が高く，ATR症例の検出に有用であり，本法により原因不明の静脈血栓塞栓症における新規血栓性素因・ATRの関与の実態が明らかとなることが期待される。

おわりに

VTEの遺伝性リスクとして様々な凝固関連因子の遺伝子異常が同定されてきたが，家族歴があり明らかに遺伝性血栓症であっても，いまだに原因遺伝子変異が不明なものがある。我々は，通常では出血傾向が予想される凝固因子・プロトロンビンの遺伝子変異が，逆に血栓傾向となる新たな血栓性素因・ATRを世界で初めて報告した。この発見は，今まで原因不明とされて来たVTEの中には少なからずATRが関与するものがあることを示すもので，事実，日本人だけでなく欧米人をはじめとして世界中で報告が見られている。今後，さらにATR症例での病態解明の研究成果が蓄積され，遺伝性血栓症においての血栓症発症予防につながる成果の得られることが期待される。

本研究の一部は，厚生労働省科学研究費補助金ならびに日本学術振興会科学研究費補助金（25293129, 25460683）で行った。

著者のCOI（conflicts of interest）開示：小嶋哲人：日当・講演料（第一三共株式会社）

文　献

1) Rosendaal F. Venous thrombosis: a multicausal disease. Lancet. 1999; **353**: 1167-1173.
2) Kimura R, Honda S, Kawasaki T, et al. Protein S-K196E mutation as a genetic risk factor for deep vein thrombosis in Japanese patients. Blood. 2006; **107**: 1737-1738.
3) Miyawaki Y, Suzuki A, Fujita J, et al. Thrombosis from a prothrombin mutation conveying antithrombin resistance. N Engl J Med. 2012; **366**: 2390-2396.
4) Simioni P, Campello E, Spiezia L. Prothrombin mutation conveying antithrombin resistance. N Engl J Med. 2012; **367**: 1069; author reply 1069-1070.
5) Egeberg O. Inherited antithrombin deficiency causing thrombophilia. Thromb Diath Haemorrh. 1965; **13**: 516-530.
6) Griffin JH, Evatt B, Zimmerman TS, Kleiss AJ, Wideman C. Deficiency of protein C in congenital thrombotic disease. J Clin Invest. 1981; **68**: 1370-1373.
7) Comp P, Esmon C. Recurrent venous thromboembolism in patients with a partial deficiency of protein S. N Engl J Med. 1984; **311**: 1525-1528.
8) Miyata T, Sato Y, Ishikawa J, et al. Prevalence of genetic mutations in protein S, protein C and antithrombin genes in Japanese patients with deep vein thrombosis. Thromb Res. 2009; **124**: 14-18.
9) Bertina RM, Koeleman BP, Koster T, et al. Mutation in blood coagulation factor V associated with resistance to activated protein C. Nature. 1994; **369**: 64-67.
10) Poort SR, Rosendaal FR, Reitsma PH, Bertina RM. A common genetic variation in the 3'-untranslated region of the prothrombin gene is associated with elevated plasma prothrombin levels and an increase in venous thrombosis. Blood. 1996; **88**: 3698-3703.
11) Simioni P, Tormene D, Tognin G, et al. X-linked thrombophilia with a mutant factor IX (factor IX Padua). N Engl J Med. 2009; **361**: 1671-1675.
12) 酒井道生, 浦野元, 飯沼麻美, 岡本 好司, 大里 敬一, 白幡 聡. 乳児期発症例を含む血栓症多発の1家系. 産業医大誌. 2001; **23**: 297-305.
13) ten Kate MK, He C, van Schouwenburg IM, et al. A genome wide linkage scan for thrombosis susceptibility genes identifies a novel prothrombin mutation [abstract]. J Thromb Haemost. 2009; **7 Suppl 2**: 237. Abstract OC-WE-098.
14) Li W, Johnson DJ, Esmon CT, Huntington JA. Structure of the antithrombin-thrombin-heparin ternary complex reveals the antithrombotic mechanism of heparin. Nat Struct Mol Biol. 2004; **11**: 857-862.
15) Takagi Y, Kato I, Ando Y, et al. Antithrombin-resistant prothrombin Yukuhashi mutation also causes thrombomodulin resistance in fibrinogen clotting but not in protein C activation. Thromb Res. 2014; **134**: 914-917.
16) Murata M, Takagi A, Suzuki A, et al. Development of a new laboratory test to evaluate antithrombin resistance in plasma. Thromb Res. 2014; **133**: 293-298.
17) 村田萌, 高木明, 岸本磨由子, ほか. 原因不明であった静脈血栓塞栓症にみられたアンチトロンビン抵抗性を示す本邦2家系目のプロトロンビン異常症[抄録]. 第33回日本臨床検査医学会東海・北陸支部例会. 2014. 20.
18) Djordjevic V, Kovac M, Miljic P, et al. A novel prothrombin mutation in two families with prominent thrombophilia—the first cases of antithrombin resistance in a Caucasian population. J Thromb Haemost. 2013; **11**: 1936-1939.
19) Sivasundar S, Oommen AT, Prakash O, et al. Molecular defect of 'Prothrombin Amrita': substitution of arginine by glutamine (Arg553 to Gln) near the Na^+ binding loop of prothrombin. Blood Cells Mol Dis. 2013; **50**: 182-183.

Antithrombin resistance: a new mechanism of inherited thrombophilia

Tetsuhito KOJIMA, Akira TAKAGI, Moe MURATA, Yuki TAKAGI

Department of Pathophysiological Laboratory Sciences, Nagoya University Graduate School of Medicine

Key words : Hereditary thrombophilia, Prothrombin Yukuhashi, Antithrombin resistance

Venous thromboembolism is a multifactorial disease resulting from complex interactions among genetic and environmental factors. To date, numerous genetic defects have been found in families with hereditary thrombophilia, but there may still be many undiscovered causative gene mutations. We investigated a possible causative gene defect in a large Japanese family with inherited thrombophilia, and found a novel missense mutation in the prothrombin gene (p.Arg596Leu) resulting in a variant prothrombin (prothrombin Yukuhashi). The mutant prothrombin had moderately lower activity than wild type prothrombin in clotting assays, but formation of the thrombin-antithrombin (TAT) complex was substantially impaired resulting in prolonged thrombin activity. A thrombin generation assay revealed that the peak activity of the mutant prothrombin was fairly low, but its inactivation was extremely slow in reconstituted plasma. The Leu596 substitution caused a gain-of-function mutation in the prothrombin gene, resulting in resistance to antithrombin and susceptibility to thrombosis. We also showed the effects of the prothrombin Yukuhashi mutation on the thrombomodulin-protein C anticoagulation system, recent development of a laboratory test detecting antithrombin resistance in plasma, and another antithrombin resistant mutation found in other thrombophilia families.

Influence of ADAMTS13 deficiency on venous thrombosis in mice

Yuko Tashima; Fumiaki Banno; Masashi Akiyama; Toshiyuki Miyata
Department of Molecular Pathogenesis, National Cerebral and Cardiovascular Center, Osaka, Japan

Dear Sirs,

Recent studies of experimental murine models of venous thrombosis revealed that neutrophils, monocytes and platelets contribute to the initiation and amplification of venous thrombosis (1–4). In the early stage of venous thrombosis, neutrophils are recruited and, upon activation, neutrophil extracellular traps (composed of DNA, histones, and granule cytotoxic enzymes) are released and a web-like extracellular network is formed on the vascular lumen. The neutrophil extracellular traps provide a scaffold for platelet adhesion and aggregation for the recruitment of red blood cells (3, 5). Monocytes are also recruited to the site of activated endothelium and are involved in fibrin formation through the intravascular expression of tissue factor (2). Activated endothelium releases unusually large von Willebrand factor (VWF) multimers from Weibel-Palade bodies that recruit circulating platelets. Since thrombi in the venous thrombosis models in VWF-deficient mice were greatly reduced, VWF multimers are important for the recruitment of platelets and essential for thrombus formation (1).

Correspondence to:
Toshiyuki Miyata
Department of Molecular Pathogenesis
National Cerebral and Cardiovascular Center
5–7–1, Fujishirodai, Suita, Osaka, 565–8565, Japan
Tel.: +81 6 6833 5012, Fax: +81 6 6835 1176
E-mail: miyata@ncvc.go.jp

Financial support:
This work was supported in part by grants-in-aid from the Ministry of Health, Labour, and Welfare of Japan; from the Ministry of Education, Culture, Sports, Science, and Technology of Japan; from the Japan Society for the Promotion of Science; from the Uehara Memorial Foundation; from the Takeda Science Foundation; and from the Japan Cardiovascular Research Foundation.

Received: August 6, 2014
Accepted after major revision: February 14, 2015
Epub ahead of print: April 9, 2015

http://dx.doi.org/10.1160/TH14-08-0656
Thromb Haemost 2015; 114: 206–207

The platelet binding to VWF is negatively regulated by a plasma VWF-cleaving protease, ADAMTS13. We and others have previously demonstrated that ADAMTS13-deficient mice do not show any evidence of thrombocytopenia, haemolytic anaemia, or microvascular thrombosis, although unusually large VWF multimers were detected in their plasma (6–8). As ADAMTS13 reduces the size of VWF multimers, thereby decreasing their thrombogenic potential, we hypothesised that ADAMTS13 deficiency could cause an excess recruitment of platelets on VWF multimers and result in an aggravation of venous thrombosis. To test whether ADAMTS13 deficiency promotes thrombus formation, we induced venous thrombosis in ADAMTS13-defficient mice using the electrolytic inferior vena cava (IVC) model (4, 9).

All mice used in this study were 9– to 12-week-old males with the 129/Sv genetic background (7, 10). Mice were anesthetised by an intraperitoneal administration of 2,2,2-tribromoethanol (375 mg/kg). A ventral midline incision (2 cm) was made with iris scissors to expose the IVC. All side branches of IVC were ligated with 7–0 sutures (Alfresa, Osaka, Japan). A 27-G stainless-steel needle (Nihon Koden, Tokyo, Japan) was inserted into the IVC (anode) and another needle was inserted subcutaneously (cathode). Electrolytic stimulation at a current of 100 or 200 microamperes (μAmp) was applied for 10 minutes (min) using a stimulator and a constant current unit (Nihon Koden). After the needle was carefully removed, the incision was sewn shut. The mice were observed under a heating lamp for 1–2 hours after the surgery, and then returned to their housing units. Two days later, blood was collected from the heart into sodium citrate (final concentration, 0.38%). Platelets were counted using an automated analyzer, KX-21NV (Sysmex, Kobe, Japan). The thrombi including blood vessels were excised and weighed. To examine therapeutic effects of ADAMTS13, we prepared recombinant human ADAMTS13 (rhADAMTS13) that spans from the metalloprotease domain to the spacer domain (amino acid residues 75–685), as described previously (11, 12). The activity was assessed by the FRETS-VWF73 assay (13). Immediately after the surgery, rhADAMTS13 (2,600 U/kg) was injected intravenously. All animal procedures were approved by the Animal Care and Use Committees of the National Cerebral and Cardiovascular Center. Statistical significance was assessed by the Kruskal-Wallis test and the Mann-Whitney test. P-values less than 0.05 were considered significant.

In the electrolytic IVC model, an applied direct current generates free radicals, which results in endothelial cell activation without denudation. This model produces a nonocclusive and consistent IVC thrombi under preserved blood flow (4, 9). When thrombosis was induced by the electrolytic stimulation at 100 μAmp for 10 min, the ADAMTS13-deficient mice (n = 15) showed larger thrombi compared to the wild-type (WT) mice (n = 13) 2 days after the stimulation (▶Figure 1). The thrombus weights of the ADAMTS13-deficient mice (10.9 ± 8.4 mg, mean ± SD) and WT mice (5.6 ± 4.4 mg) were significantly different (p = 0.02). Intravenous injection of rhADAMTS13 improved accelerated thrombus formation in the ADAMTS13-deficient mice (▶Figure 1). The thrombus weights of the ADAMTS13-deficient mice were significantly reduced (p = 0.008) by rhADAMTS13 injection (4.8 ± 4.2 mg, n = 9) to become comparable to those of WT mice (no infusion: 5.6 ± 4.4 mg, n = 13; + rhADAMTS13: 4.0 ± 3.2 mg, n = 8). Thus, our data indicate that ADAMTS13 deficiency is a sufficient trigger for exacerbating venous thrombosis.

The ADAMTS13-deficient mice have normal platelet counts before surgery as described previously (7, 10). The number of platelets was not different between WT and the ADAMTS13 deficient mice on two days after the electrolytic stimulation at 100 μAmp for 10 min (data not shown). When the stimulation was increased to

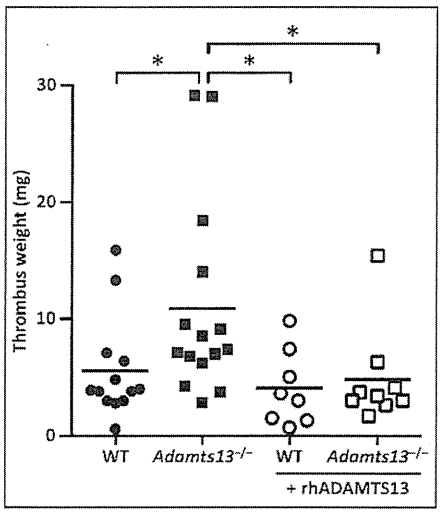

Figure 1: ADAMTS13-deficient mice showed enhanced thrombus formation in an electrolytic venous thrombosis model. Thrombosis was induced at a current of 100 µAmp for 10 min within inferior vena cava. Two days after the electrolytic stimulation, thrombi were excised and weighed. Symbols represent data from a single mouse. Bars represent the mean values of groups. WT (●), 5.6 ± 4.4 mg, mean ± SD, n = 13; *Adamts13*$^{-/-}$ (ADAMTS13 deficient mice) (■), 10.9 ± 8.4 mg, n = 15; WT + rhADAMTS13 (○), 4.0 ± 3.2 mg, n = 8; *Adamts13*$^{-/-}$ + rhADAMTS13 (□), 4.8 ± 4.2 mg, n = 9. *Significant differences at $p < 0.05$ in comparison with the *Adamts13*$^{-/-}$ group by the Mann-Whitney test.

200 µAmp for 10 min, the number of platelets in the ADAMTS13-deficient mice was greatly decreased (WT mice, 41.1 ± 19.4 × 10^4 platelets/µl, n = 9; ADAMTS13-deficient mice, 15.3 ± 8.8 × 10^4 platelets/µl, n = 6; p = 0.006). However, the ADAMTS13-deficient mice were prone to die before the second day after the stimulation (death rate: three-ninth). Lethal thrombotic embolisation might be induced in the ADAMTS13-deficient mice after the strong electrolytic stimulation.

In humans, the low-dose administration of aspirin in patients with unprovoked venous thrombosis who had discontinued anticoagulant treatment reduced the risk of recurrence (14). A recent next-generation sequencing study identified an excess of rare coding single-nucleotide variants of the *ADAMTS13* gene in patients with deep-vein thrombosis with the relative risk 1.5–5.0 (15). These studies indicated that platelets have an important role in the development of venous thrombosis in humans, and our finding that ADAMTS13-deficient mice with unusually large VWF multimers developed greater IVC thrombosis compared to wild-type mice supports these studies.

The results of the present study demonstrate that the deficiency of ADAMTS13 results in increased formation of venous thrombosis in mice. We and other groups have previously observed that ADAMTS13 deficiency in mice exacerbates focal cerebral ischaemia (16–18) and acute myocardial ischaemia/reperfusion injury (12, 19, 20). Taken together, the relevant data suggest that ADAMTS13 functions to reduce the size of not only arterial thrombi but also venous thrombi *in vivo*. Our data suggest that ADAMTS13 contributes to protect platelet-mediated thrombus development in venous thrombosis.

Acknowledgements
We thank Koichi Kokame (National Cerebral and Cardiovascular Center) for the useful discussion.

Conflicts of interest
None declared.

References

1. Brill A, Fuchs TA, Chauhan AK, et al. von Willebrand factor-mediated platelet adhesion is critical for deep vein thrombosis in mouse models. Blood 2011; 117: 1400–1407.
2. von Bruhl ML, Stark K, Steinhart A, et al. Monocytes, neutrophils, and platelets cooperate to initiate and propagate venous thrombosis in mice in vivo. J Exp Med 2012; 209: 819–835.
3. Fuchs TA, Brill A, Wagner DD. Neutrophil extracellular trap (NET) impact on deep vein thrombosis. Arterioscler Thromb Vasc Biol 2012; 32: 1777–1783.
4. Diaz JA, Hawley AE, Alvarado CM, et al. Thrombogenesis with continuous blood flow in the inferior vena cava. A novel mouse model. Thromb Haemost 2010; 104: 366–375.
5. Fuchs TA, Brill A, Duerschmied D, et al. Extracellular DNA traps promote thrombosis. Proc Natl Acad Sci USA 2010; 107: 15880–15885.
6. Motto DG, Chauhan AK, Zhu G, et al. Shigatoxin triggers thrombotic thrombocytopenic purpura in genetically susceptible ADAMTS13-deficient mice. J Clin Invest 2005; 115: 2752–2761.
7. Banno F, Kokame K, Okuda T, et al. Complete deficiency in ADAMTS13 is prothrombotic, but it alone is not sufficient to cause thrombotic thrombocytopenic purpura. Blood 2006; 107: 3161–3166.
8. Banno F, Chauhan AK, Miyata T. The function of ADAMTS13 in thrombogenesis in vivo: insights from mutant mice. Int J Hematol 2010; 91: 30–35.
9. Diaz JA, Alvarado CM, Wrobleski SK, et al. The electrolytic inferior vena cava model (EIM) to study thrombogenesis and thrombus resolution with continuous blood flow in the mouse. Thromb Haemost 2013; 109: 1158–1169.
10. Banno F, Chauhan AK, Kokame K, et al. The distal carboxyl-terminal domains of ADAMTS13 are required for regulation of in vivo thrombus formation. Blood 2009; 113: 5323–5329.
11. Akiyama M, Takeda S, Kokame K, et al. Crystal structures of the noncatalytic domains of ADAMTS13 reveal multiple discontinuous exosites for von Willebrand factor. Proc Natl Acad Sci USA 2009; 106: 19274–19279.
12. Doi M, Matsui H, Takeda H, et al. ADAMTS13 safeguards the myocardium in a mouse model of acute myocardial infarction. Thromb Haemost 2012; 108: 1236–1238.
13. Kokame K, Nobe Y, Kokubo Y, et al. FRETS-VWF73, a first fluorogenic substrate for ADAMTS13 assay. Br J Haematol 2005; 129: 93–100.
14. Becattini C, Agnelli G, Schenone A, et al. Aspirin for preventing the recurrence of venous thromboembolism. N Engl J Med 2012; 366: 1959–1967.
15. Lotta LA, Tuana G, Yu J, et al. Next-generation sequencing study finds an excess of rare, coding single-nucleotide variants of ADAMTS13 in patients with deep vein thrombosis. J Thromb Haemost 2013; 11: 1228–1239.
16. Zhao BQ, Chauhan AK, Canault M, et al. von Willebrand factor-cleaving protease ADAMTS13 reduces ischemic brain injury in experimental stroke. Blood 2009; 114: 3329–3334.
17. Fujioka M, Hayakawa K, Mishima K, et al. ADAMTS13 gene deletion aggravates ischemic brain damage: a possible neuroprotective role of ADAMTS13 by ameliorating postischemic hypoperfusion. Blood 2010; 115: 1650–1653.
18. Khan MM, Motto DG, Lentz SR, et al. ADAMTS13 reduces VWF-mediated acute inflammation following focal cerebral ischemia in mice. J Thromb Haemost 2012; 10: 1665–1671.
19. De Meyer SF, Savchenko AS, Haas MS, et al. Protective anti-inflammatory effect of ADAMTS13 on myocardial ischemia/reperfusion injury in mice. Blood 2012; 120: 5217–5223.
20. Gandhi C, Khan MM, Lentz SR, et al. ADAMTS13 reduces vascular inflammation and the development of early atherosclerosis in mice. Blood 2012; 119: 2385–2391.

PLOS | ONE

RESEARCH ARTICLE

ELISA-Based Detection System for Protein S K196E Mutation, a Genetic Risk Factor for Venous Thromboembolism

Keiko Maruyama[1☯], Masashi Akiyama[1☯], Koichi Kokame[1], Akiko Sekiya[2], Eriko Morishita[2], Toshiyuki Miyata[1]*

1 Department of Molecular Pathogenesis, National Cerebral and Cardiovascular Center, Suita, Japan, **2** Department of Clinical Laboratory Sciences, Graduate School of Medical Science, Kanazawa University, Kanazawa, Japan

☯ These authors contributed equally to this work.
* miyata@ncvc.go.jp

Citation: Maruyama K, Akiyama M, Kokame K, Sekiya A, Morishita E, Miyata T (2015) ELISA-Based Detection System for Protein S K196E Mutation, a Genetic Risk Factor for Venous Thromboembolism. PLoS ONE 10(7): e0133196. doi:10.1371/journal.pone.0133196

Editor: Pablo Garcia de Frutos, IIBB-CSIC-IDIBAPS, SPAIN

Received: November 24, 2014

Accepted: June 23, 2015

Published: July 17, 2015

Data Availability Statement: All relevant data are within the paper.

Funding: This work was supported in part by grants-in-aid from the Ministry of Health, Labour and Welfare of Japan, the Japan Society for the Promotion of Science, and the Takeda Science Foundation.

Competing Interests: The authors have declared that no competing interests exist.

Abstract

Protein S (PS) acts as a cofactor for activated protein C in the plasma anticoagulant system. PS Lys196-to-Glu (K196E) mutation is a genetic risk factor for venous thromboembolism in Japanese individuals. Because of the substantial overlap in PS anticoagulant activity between KK (wild-type) and KE (heterozygous) genotypes, it is difficult to identify PS K196E carriers by measuring PS activity. Here, we generated monoclonal antibodies specific to the PS K196E mutant and developed a simple and reliable method for the identification of PS K196E carriers. We immunized mice with a keyhole limpet hemocyanin-conjugated synthetic peptide with Glu196. The hybridoma cells were screened for the binding ability of the produced antibodies to recombinant mutant EGF-like domains of PS (Ile117–Glu283). We obtained three hybridoma cell lines producing PS K196E mutation-specific antibodies. We established a sandwich enzyme-linked immunosorbent assay (ELISA) system in which the PS K196E mutation-specific monoclonal antibody was used as a detection antibody. We measured human plasma samples by using this system and successfully discriminated 11 individuals with the KE genotype from 122 individuals with the KK genotype. The ELISA system using the PS K196E mutation-specific antibody is a useful tool for the rapid identification of PS K196E carriers, who are at a higher risk for venous thromboembolism.

Introduction

Protein S (PS) is an anticoagulant protein that acts as a cofactor for activated protein C in the proteolytic inactivation of activated coagulation factors Va and VIIIa and as a cofactor for tissue factor pathway inhibitor to efficiently inhibit factor Xa [1–4]. Thus, the reduced PS anticoagulant activity observed in congenital PS deficiency is a genetic risk for venous thromboembolism (VTE). PS circulates in human plasma at a concentration of approx. 25 μg mL^{-1} (~350 nM).